

NUCLEOCYTOPLASMIC MOVEMENT OF FLUORESCENT TRACERS MICROINJECTED INTO LIVING SALIVARY GLAND CELLS

PHILIP L. PAINE. From the Laboratory of Cell Physiology, Department of Biology, Michigan Cancer Foundation, Detroit, Michigan 48201 and the Department of Physiology and Biophysics, University of Miami School of Medicine, Miami, Florida 33152

Many molecules, including macromolecules, cross the nuclear envelope in the course of nucleocytoplasmic exchange. Work with fluorescent and radioactively labeled proteins microinjected into the cytoplasm showed that proteins with diameters less than 30–40 Å pass from the cytoplasm to the nucleus much more rapidly than molecules with diameters of 60–70 Å, which are delayed at the level of the nuclear envelope. These results were obtained by autoradiographic and fluorescence microscope analysis of sectioned oocytes of frogs (*Xenopus laevis*) (4) and cockroaches (*Periplaneta americana*) (15). Recently, a quantitative ultra-low

temperature autoradiographic study of the nuclear entry of [³H]dextran in mature oocytes of *Rana pipiens* has provided the basis for a restricted-diffusion model of nucleocytoplasmic exchange through nuclear pores with patent radii of about 45 Å (16). The present paper extends the study of nucleocytoplasmic passage of macromolecules to a somatic cell, the giant larval salivary gland cell of *Chironomus thummi*. Fluorescent tracers were injected into the cytoplasm or the nucleus, and their movements followed within the *living cell* by dark field observation, while the cell state was electrophysiologically monitored.

MATERIALS AND METHODS

Salivary glands from mid 4th instar, late 4th instar, and early prepupal larvae were isolated and immobilized on the bottom of a Petri dish in physiological medium (17). The gland morphology has been described by Rose (19) and the cell ultrastructure and cytochemistry by Laufer (9), Rose (19), and Stevens and Swift (20). The cell width is approximately 100 μm , its length about 120 μm , and the nuclear diameter about 50 μm . In the position of the isolated gland preparation, the nucleus is over- and underlaid by layers of cytoplasm estimated to be less than 10 μm thick. The nucleus and the cytoplasm are rather translucent; because of the size and transparency of the cell and nucleus, it is easy to see pipette tips in the nucleus or cytoplasm, and intracellular fluorescent tracer movement is readily observable (Fig. 1).

Experiments were performed at a magnification of 400. Micropipette insertion was done in bright field, while microinjection of the fluorescent tracer and subsequent observation was done in dark field with an HBO 200 mercury arc source, a BG12 exciter filter, and a gelatin barrier filter (500-nm cutoff). The tracers were hydraulically injected through micropipettes of 2–4 μm tip diameter. The injected volume was less than 10 nl (about 1% of the cell volume), as determined by pipette calibrations with tritiated water of known activity. Injections into the cytoplasm were done between the basal cell border and the nucleus, with care being taken not to touch the nucleus.

Before injection the cytoplasm has a low level of autofluorescence and is visible against the dark field background; the nucleus has less autofluorescence, and appears as dark as the background. The fluorescent tracer is visible in the pipette tip. Each injection pulse puts a visible puff of tracer into the cell; after injection the tracer is seen by its fluorescence within the cell (Fig. 1 *b, c, and f*).

The tracers used are listed in Table I. Proteins were conjugated with fluorescein isothiocyanate (FITC) by a dialysis exchange technique; the conjugates were previously tested for retention of their native molecular conformations and electrical charges (15). Tracers were injected in a solution of 180 mM KCl, 1 mM KH_2PO_4 , and 2 mM NaHCO_3 (FITC proteins, 1–3%; Na-fluorescein and FITC, 0.02%; poly N^s L-glutamine, 4%; all wt/vol).

The nucleus is large compared to the cytoplasm of these cells, and there is little cytoplasm in the optical path above or below the nucleus. Observation of the relative fluorescence intensities of the nuclear and cytoplasmic compartments thus closely reflects the relative concentrations (volume basis) of fluorescent materials within these compartments. This point is illustrated by the following observations: nuclei of uninjected cells appear as black as the dark field background, even though the cytoplasm exhibits autofluorescence; and the nuclei of cells cytoplasmically injected with brightly fluorescent tracers, which spread throughout the cytoplasm within

seconds but only slowly enter the nucleus, appear as dark as the background until fluorescent tracer enters the nucleus.

The cell membrane potential and electrical coupling between the injected cell and an adjacent cell (13) were continuously monitored with microelectrodes during and after tracer injection. Maintenance of initial cell resting potential (typically 30–50 mV) and electrical coupling were the acceptance criteria of the experiments. An additional criterion was morphological. A damaged cell goes through a series of visible changes: cytoplasmic granulation, followed by nuclear swelling and chromosome condensation within minutes after the loss of its membrane potential. In some experiments (see Table I) the electrical monitoring was omitted, and normal morphology was the only acceptance standard; the cells in these experiments probably had normal cell membrane potentials, but there is no assurance that they were electrically coupled.

RESULTS AND DISCUSSION

After injection into the cytoplasm, tracer fluorescence spreads from the injection site throughout the cytoplasm and into the nucleus. The smaller molecules, fluorescein, FITC, and polyglutamine, enter the nucleus rapidly, the fluorescence contributed by these molecules inside the nucleus matching sensibly that of the cytoplasm within seconds (Table I). Very rapid nuclear entry of Na-fluorescein and FITC is consistent with measurements of Kohen et al. (8) in tissue culture cells, showing that the glycolytic substrates glucose-6-phosphate and glucose-1-phosphate (mol wt 259) move across the nuclear envelope in a fraction of 1 s. Rapid entry of FITC into nuclei has been observed in roach oocytes (15), and Na-fluorescein enters the nuclei of in vitro cultured cells: rat liver and fibroblast cells, rat hepatoma cells, human fibroblasts, and rabbit lens cells (R. Azarnia, personal communication). The nuclear entry rate of polyglutamine is closer to that of Na-fluorescein and FITC than that of the proteins (Table I).

The larger molecules, bovine serum albumin (BSA), ovalbumin, horseradish peroxidase (HRP), myoglobin, and cytochrome *c*, penetrate less readily into the nucleus; when they are injected into the cytoplasm close to the nucleus (less than $\approx 30 \mu\text{m}$), their fluorescence spreads to the nucleus and rebounds back from the nuclear surface toward the injection pipette. This phenomenon is not observed with the smaller molecules. The fluorescence then enters into the nucleus, at rates which decrease with increasing tracer molecular size. The nuclear fluorescence intensities of myoglobin and cyto-

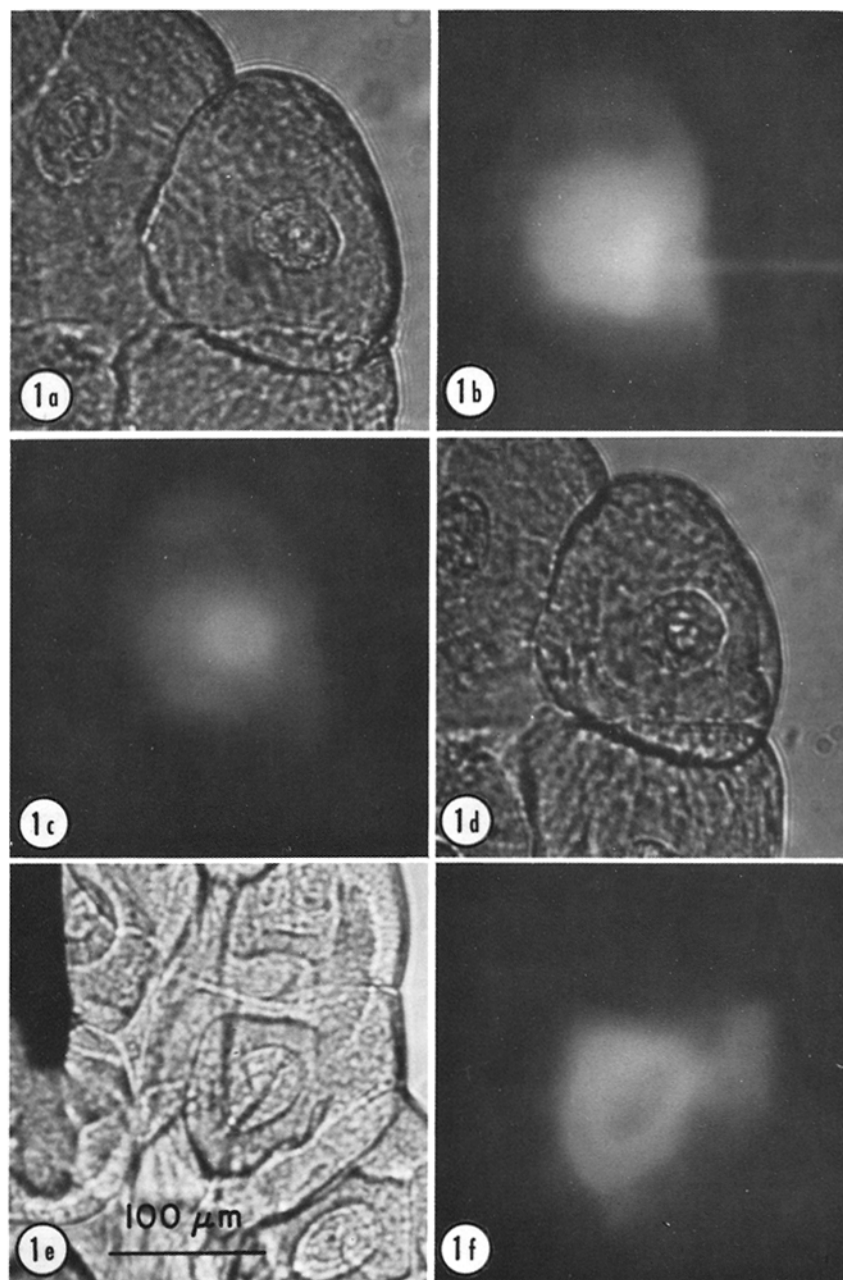


FIGURE 1 Bright field and dark field fluorescence micrographs of a portion of a salivary gland during a typical experiment with cytoplasmic microinjection of FITC-myoglobin: (a) bright field immediately before impalement and injection ($t = 0$ min); (b) fluorescence of the FITC-myoglobin in the injection pipette and the injected cell (film exposure was $t = 0-2$ min); (c) fluorescence image at $t = 20-22$ min (pipette withdrawn), a similar image, with nuclear fluorescence greater than cytoplasmic, was observed as early as $t =$ min; (d) bright field picture at $t = 45$ min, the cell shows a slight dimple remaining at the site of pipette penetration, but appears healthy. (e, f) Micrographs taken 20 min after cytoplasmic injection of FITC-BSA: (e) bright field, dark object is tip of stainless steel pin used to immobilize gland; (f) fluorescence, a similar image, with nuclear fluorescence less than cytoplasmic, was observed as late as $t = 3$ h. All micrographs $\times 220$.

TABLE I
Nucleocytoplasmic Tracer Movement

Tracer (size*)	Nucleocytoplasmic Fluorescence Equalization Time†		Number of Experiments‡	
	Cytoplasmic Injection	Nuclear Injection	Cytoplasmic Injection	Nuclear Injection
BSA (radius = 35 Å)	> 3 h	—	7 (3,4)	—
Ovalbumin (radius = 27 Å)	> 40 min	> 30 min	3 (1,2)	4 (0,4)
HRP (radius = 24 Å)	5–25 min	> 10 min	4 (1,3)	1 (0,1)
Myoglobin (43 × 35 × 23 Å)	< 3 min	< 3 min	8 (5,3)	3 (1,2)
Cytochrome <i>c</i> (34 × 34 × 30 Å)	< 3 min	< 3 min	1 (1,0)	1 (0,1)
Poly N ⁵ L-glutamine ¶ (mol wt 4,200)	s	—	12 (8,4)	—
FITC (mol wt 389)	s	—	3 (3,0)	—
Na-fluorescein (mol wt 376)	s	—	4 (3,1)	—

* See Paine and Feldherr (15) for more data and references on molecular characteristics.

† The time after microinjection required for the observed fluorescence intensity in the uninjected compartment (nucleus or cytoplasm) to become equal to the intensity in the injected compartment.

‡ Total number (number with electrical acceptance criteria, number with only morphological criteria). See text for explanation of criteria.

|| This is the time for observable fluorescence to appear in the cytoplasm; with nuclear injections of myoglobin, the cytoplasmic fluorescence was never seen to equal the nuclear (see text).

¶ Custom synthesis of FITC-poly N⁵ (3-hydroxy propyl) L-glutamine by Miles-Yeda, Ltd., Kiryat Weizmann, Rehovoth, Israel.

chrome *c* approach those of the cytoplasm within less than 3 min (Fig. 1 *b*), and within 5 min the myoglobin fluorescence level in the nucleus is greater than the cytoplasmic level (Fig. 1 *c*).¹ Horseradish peroxidase takes up to 25 min to reach nuclear fluorescence equal to the cytoplasmic fluorescence, and nuclear levels of ovalbumin and BSA fluorescence do not approach the cytoplasmic even after 40 min and 3 h, respectively (see Fig. 1 *f* and Table I).

The inverse relationship of nuclear entry rates to molecular size in the salivary gland cell is similar to that observed in cockroach oocytes with the same fluorescently labeled proteins (15). (Similarity of the nuclear to cytoplasmic volume ratios of

these cell types allows direct comparison of rates.) In the roach oocyte the relationship is exponential and asymptotes at 90–100 Å; tracers larger than 100 Å in diameter do not significantly enter the nucleus. The size dependence of protein movement in the amphibian oocyte is similar (1, 4). While rate constants for protein movement in any cell are not available, they are available for the nuclear entry of [³H]dextran in amphibian oocytes (16). These are accounted for by a model of restricted diffusion through 45 Å radius nuclear pores. The similarity exhibited by nucleocytoplasmic tracer protein movement in the three cell types implies that the 45-Å pore of the amphibian oocyte may provide a good estimate of pore radius in cockroach oocytes and salivary gland cells as well.

After injection of HRP, ovalbumin, myoglobin, or cytochrome *c* into the nucleus, the time course of tracer spread to the cytoplasm is similar to the cytoplasm to nucleus results (see Table I). This isotropy is consistent with envelope permeation by restricted diffusion through pores with patent radii

¹ Similar nuclear excesses (above cytoplasmic levels) of myoglobin (15) and other exogenous tracers (histones [4], dextrans [16], colloidal gold [2], and small tracers [5, 11, 14]) have been reported in oocytes, amebas, and neurons. This phenomenon can be attributed to solute exclusion by the cytoplasm (5, 16).

of about 45 Å. This implies that the nucleocytoplasmic transport of ribonucleoprotein particulates (radii ≥ 200 Å [20]) employs special nondiffusional mechanisms at the level of the nuclear envelope. Our results seem to require that the particulates and/or envelope pore complexes undergo conformational changes during transit through the envelope. Morphological evidence for such changes exists (20).

Loewenstein and co-workers (6, 11) found nuclear envelope electrical resistances, R_T in *C. thummi* and *Drosophila flavorapleta* larval salivary gland cells, of 0.5–2.0 Ω cm². Similar measurements in immature oocytes (< 350 μ m diameter) of several amphibians (10) gave R_T -values less than 0.001 Ω cm². These differences are not attributable to ultrastructural differences among the nuclei (21) and have remained unexplained and somewhat perplexing. The salivary gland cell envelope resistance has been widely interpreted to mean that the envelope of this cell is a formidable barrier to ion movement, and by implication to the movement of large solutes. This interpretation, coupled with the fact that considerable macromolecular traffic between nucleus and cytoplasm exists, has led to the assumption by some that the permeability of the immature oocyte nuclear envelope is representative of most cells, while that of the salivary gland cell envelope is atypical and requires explanation. The present tracer studies suggest otherwise, that salivary gland cell nuclear envelope permeability is similar to that of other cells and consistent with patent pore radii of about 45 Å. Hence, a discrepancy may seem to exist between macromolecular fluxes observed by us and the electrical resistances measured by Loewenstein et al. (6, 11). This can be shown not to be the case.

Assuming the salivary gland cell nuclear envelope pore complex to have a patent channel with radius (r) of 45 Å and length (d) of 1,500 Å (16), and the specific resistivity (ρ) of the channel contents to be about that of cytoplasm, 100 Ω cm (12), the resistance (R_p) of a pore complex is

$$R_p = \frac{\rho[1 + 1.64(r/d)]d}{\pi r^2(l-a/r)^6} = 3.25 \times 10^9 \Omega, \quad (1)$$

where a , the hydrated radius of the current carrying ions, is taken as 2.0 Å. (This approximation [18] does not take into account electrostatic interactions between pores. Kanno and Loewenstein [7]

showed that a neglect of this sort introduces only a very small error.) Further, assuming that one-half of the pores are plugged with RNP in transit from nucleus to cytoplasm (3), the density of patent nuclear pores (N) is about 5.78×10^9 cm² (21). Then the calculated envelope resistance, $R_T = R_p/N = 0.56 \Omega$ cm², is on the order of the measured values. We conclude that both the measured nuclear envelope resistance, R_T , and the fluorescent tracer kinetics in salivary gland cells are consistent with 45 Å radius pores.

The absence of a measurable R_T in immature amphibian oocytes remains unexplained. It could be due to unrecognized technical difficulties or may reflect a considerably higher nuclear envelope permeability in these cells than in salivary gland cells and mature oocytes. In either case, no significant disparity appears to exist between the observed electrical and permeability properties of the salivary gland cell nuclear envelope.

SUMMARY

The permeability of the nuclear envelope of a somatic cell, the *C. thummi* larval salivary gland cell, was studied by intracellular microinjection of fluorescent molecular tracers. As shown previously in oocytes (4, 5, 15, 16), the envelope is permeable to a wide variety of materials, including molecules which are large enough to possess considerable biological specificities and to play important roles in regulation of cellular activities. The envelope exhibits transport selectivity on the basis of size in the range of naturally occurring intracellular materials and it may thus perform important controlling functions in nucleocytoplasmic exchange. The nucleus to cytoplasm movement of in vivo ribonucleoprotein particulates in these synthetically active cells probably requires conformational changes in the particulates and/or the envelope pore complexes; morphological evidence exists for such processes in these cells (20).

My sincere thanks are extended to Professor W. R. Loewenstein and Drs. Birgit Rose, Roobik Azarnia, Samuel B. Horowitz, and Karl Magleby for their assistance in this work.

This work was supported by United States Public Health Service Research Grant CA 14464, National Science Foundation grants GB 36763X1 and GB 36005, National Institutes of Health grant GM 19548, a Damon Runyon fellowship grant DRF-699, and by an institutional grant to the Michigan Cancer Foundation from the United Foundation of Greater Detroit.

Received for publication 9 December 1974, and in revised form 27 May 1975.

REFERENCES

1. BONNER, W. M. 1975. Protein migration into nuclei. *J. Cell Biol.* **64**:421-430.
2. FELDHERR, C. M. 1972. Structure and function of the nuclear envelope. In *Advances in Cell and Molecular Biology*. E. J. DuPraw, editor. Academic Press, Inc., New York. **2**:273-307.
3. FRANKE, W. W. and U. SCHEER. 1970. The ultrastructure of the nuclear envelope of amphibian oocytes: a reinvestigation. II. The immature oocyte and dynamic aspects. *J. Ultrastruct. Res.* **30**:317-327.
4. GURDON, J. B. 1970. Nuclear transplantation and the control of gene activity in animal development. *Proc. R. Soc. Lond. B. Biol. Sci.* **176**:303-314.
5. HOROWITZ, S. B., and L. C. MOORE. 1974. The nuclear permeability, intracellular distribution, and diffusion of inulin in the amphibian oocyte. *J. Cell Biol.* **60**:405-415.
6. ITO, S., and W. R. LOEWENSTEIN. 1965. Permeability of a nuclear membrane: changes during normal development and changes induced by growth hormone. *Science (Wash. D. C.)*. **150**:909-910.
7. KANNO, Y., and W. R. LOEWENSTEIN. 1963. A study of the nucleus and cell membranes of oocytes with an intra-cellular electrode. *Exp. Cell Res.* **31**:149-166.
8. KOHEN, E., G. SIEBERT, and C. KOHEN. 1971. Transfer of metabolites across the nuclear membrane. *Hoppe-Seyler's Z. Physiol. Chem.* **352**:927-937.
9. LAUFER, H. 1963. Hormones and the development of insects. *Proc. 16th Int. Congr. Zool.* **4**:215-220.
10. LOEWENSTEIN, W. R. 1964. Permeability of the nuclear membrane as determined with electrical methods. *Protoplasmatologia*. **2**:26-34.
11. LOEWENSTEIN, W. R. and Y. KANNO. 1963. Some electrical properties of a nuclear membrane examined with a microelectrode. *J. Gen. Physiol.* **46**:1123-1140.
12. LOEWENSTEIN, W. R., Y. KANNO, and S. ITO. 1966. Permeability of nuclear membranes. *Ann. N. Y. Acad. Sci.* **137**:708-716.
13. LOEWENSTEIN, W. R., M. NAKAS, and S. J. SOCOLAR. 1967. Junctional membrane uncoupling. *J. Gen. Physiol.* **50**:1865-1891.
14. NICHOLSON, C. and S. B. KATER. 1973. In *Intracellular Staining in Neurobiology*. S. B. Kater and C. Nicholson, editors. Springer-Verlag, New York Inc. 1-20.
15. PAINE, P. L., and C. M. FELDHERR. 1972. Nucleocytoplasmic exchange of macromolecules. *Exp. Cell Res.* **74**:81-98.
16. PAINE, P. L., L. C. MOORE, and S. B. HOROWITZ. 1975. Nuclear envelope permeability. *Nature (Lond.)*. **254**:109-114.
17. POLITOFF, A., S. J. SOCOLAR, and W. R. LOEWENSTEIN. 1967. Metabolism and the permeability of cell membrane junctions. *Biochim. Biophys. Acta.* **135**:791-793.
18. QUINN, J. A., J. L. ANDERSON, W. S. HO, and W. J. PETZNY. 1972. Model pores of molecular dimension. *Biophys. J.* **12**:990-1007.
19. ROSE, B. 1971. Intercellular communication and some structural aspects of membrane junctions in a simple cell system. *J. Membr. Biol.* **5**:1-19.
20. STEVENS, B. J., and H. SWIFT. 1966. RNA transport from nucleus to cytoplasm in *Chironomus* salivary glands. *J. Cell Biol.* **31**:55-77.
21. WEINER, J., D. SPIRO, and W. R. LOEWENSTEIN. 1965. Ultrastructure and permeability of nuclear membranes. *J. Cell Biol.* **27**:107-117.